Automated Evaluation of Anisotropic Friction Pads

Anastázie Rišková, Jiří Kubík, Jan Faigl
Faculty of Electrical Engineering, Czech Technical University, Czechia
{*riskoana, kubikji2, faiglj*}*@fel.cvut.cz*

1 Introduction

Inchworms use their limbs for locomotion with two alternating locomotion pattern phases: anchoring a body part to the terrain (*anchoring* phase) and moving it forward (*sliding* phase). The presented work is motivated by such locomotion using anisotropic friction to achieve a unidirectional movement of the designed robotic inchworm depicted in Fig. 1. Existing friction anisotropy implementations include usage of active stiff materials [1, 2], kirigami-inspired structures [3], combination of soft and stiff materials [4], weight-dependent anchoring of soft scales [5]. Besides, rigid static scales [6], custom-made gel creating variable friction [7], and passive scales utilizing 3D printing with stainless steel [8] are reported in the literature.

Figure 1: The considered robot resembles an inchworm with designed anisotropic friction pads with flexible scales for anchoring.

We propose 3D-printable flexible scales using commonly available materials, avoiding the need for specialized fabrication and offering easy reproduction. Flexibility offers better adaptation to rough terrain compared to rigid scales while preserving desired frictional behavior. The proposed approach, like existing methods, depends on sufficient scale-to-surface friction, which may be compromised on smooth surfaces. In those cases, exotic materials such as custom gels may prove more effective. In this paper, we report on the testbeds developed from off-the-shelf instrumentation for the automated evaluation of the manufactured flexible anisotropic friction pads on inchworm robots.

2 Inchworm-like Robot with Anisotropic Friction Pads

The employed inchworm-like robot has 4 degrees of freedom kinematic chain, allowing one-dimensional locomotion with two friction pads at its ends. The friction pads consist of artificial 3D-printed scales placed in rigid cases made of PETG (Polyethylene Terephthalate Glycol) filament (Prusament, Czechia) as depicted in Fig. 2. The scales are arranged in rows that bend and interlock with the terrain during the anchoring phase when forces are applied in the backward direction (Fig. 2b) and press against the robot body during the sliding phase when forward motion occurs (Fig. 2c). The scales are manufactured using a flexible filament (Fiberlogy FiberFlex 40D, Poland) with a shore hardness of 40D, balancing structural integrity and flexibility. The parameters (scale thickness, scale length, and scale spacing shown in Fig. 2a) values were determined using several prototypes as parameter optimization is out of the scope of this paper and left for future extensions.

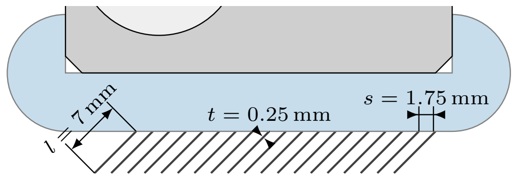

(a) Developed parameters of scales

(b) Backward movement **(c)** Forward movement

Figure 2: Developed scales parameters and working principle.

3 Evaluation of Anisotropic Friction Pads

The friction of the manufactured scales is based on measurements of static and dynamic friction between the pads and terrain surfaces, where we assume the dynamic friction coefficient is a function of the velocity $\mu(v)$. Friction has been measured experimentally using two developed testbeds, each for three terrain surface types: *Expanded Polyethylene* (EPE, Fig. 3a), *Artificial Turf* (Artificial Grass, Fig. 3b), and *Polyethylene Terephthalate Glycol* (PETG, Fig. 3c), which were selected to exhibit a range of representative frictional properties. The EPE surface is as-

(a) EPE **(b)** Artificial Grass **(c)** PETG

Figure 3: The terrain types used in the evaluation scenarios. The shown 5 cm-long plastic object is divided to 5 mm and 2 mm segments.

sumed to offer adequate friction for the pad, while artificial grass is anticipated to provide sufficient directional friction. The PETG surface is expected to have low friction, and it is thus challenging for locomotion.

Friction is measured for scales in the forward and backward directions, denoted *soft-forward* and *soft-backward*, respectively. Moreover, a scale base material is used to evaluate terrain interlocking behavior in a scenario referred to as *soft-base*. Besides, a stiff PETG is measured to determine the plausibility of using a robot frame for locomotion, which is denoted *stiff* setup. For each test scenario, the measurements are repeated ten times.

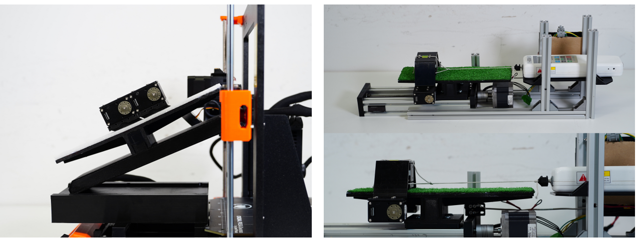

(a) Static friction testbed **(b)** Dynamic friction testbed

Figure 4: Friction measurements testbeds. The static friction testbed (left) is used to measure the angle at which the friction is no longer sufficient to keep the object in place. The dynamic friction testbed (right) directly measures the friction force while the surface moves at the desired speed.

The static friction setup consists of an inclined terrain surface and a weighted sample freely placed on the terrain; see Fig. 4a. The inclinable surface is attached to a free rotational joint that can move up and down to control the surface's slope. The gravitational force acting on the object on the inclined surface has a component parallel to the surface that pushes the object downhill and a perpendicular component that contributes to the static friction. The value of $\mu(0)$ is determined from the highest tilt angle at which the object remains motionless.

The dynamic friction setup consists of the digital force gauge (DFG) FH 100 (Kern&Sohn, Germany) and surface attached to a platform capable of horizontal movement at a constant speed. A weighted object with the friction pads is placed on the surface and attached to the DFG with Dyneema string as shown in Fig. 4b. The DFG measurements are collected for surface movements at known velocity v selected from 1–45 $\mathrm{mm\,s^{-1}}$ corresponding to the expected robot's speeds range, from which dynamic friction coefficient $\mu(v)$ is calculated. The rising edge is excluded from the data to suppress the transient response.

The results depicted in Fig. 5 support the expected properties. Terrains have less friction with the stiff robot part material (stiff) than with the scale material (soft-base). Moreover, the friction differences between forward and backward directions are the most pronounced for an EPE terrain, where the base material provides enough friction to anchor the scales. Similarly, artificial grass makes the anchoring sufficient; however, at speeds above $v = 25\,\mathrm{mm\,s^{-1}}$, significant sideways oscillations caused by lateral friction resulted

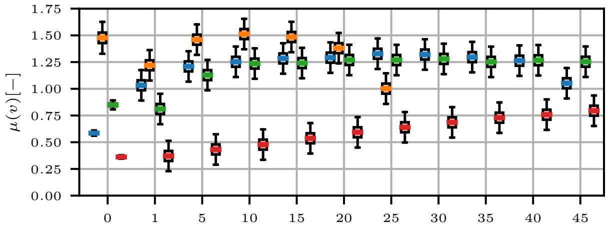

(a) EPE terrain

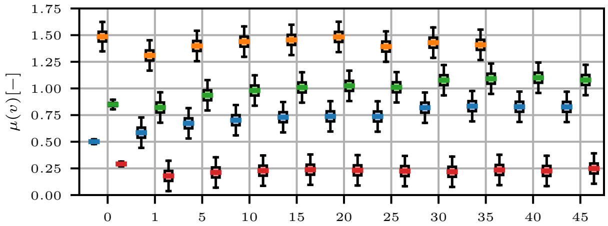

(b) Artificial grass terrain

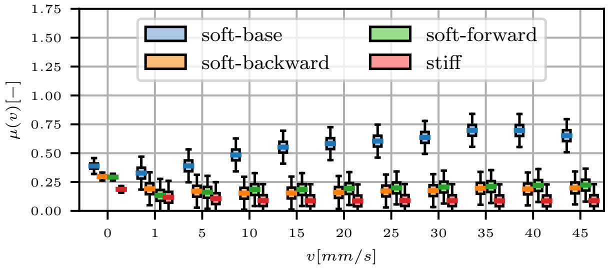

(c) PETG terrain

Figure 5: Measured friction coefficients between the terrains and the following elements: base material (*soft-base*), backward- and forward-facing scales (*soft-backward* and *soft-forward*), and the stiff material (*stiff*).

in disengagement of the scales and a decrease of the friction. Regardless of their orientation, the scales failed to engage sufficiently on the PETG terrain, supporting the expected requirement for sufficient soft-base friction.

4 Conclusion

In this paper, we report on the experimental validation of the proposed 3D-printable anisotropic friction pads evaluated on automated testbeds. The experimental results confirm friction anisotropy, resulting in a design that can be used for robot locomotion. The collected data allow the construction of a friction model for the inchworm robot to bridge the reality gap for simulation, reducing the mismatch between the simulated and real friction. Furthermore, known friction for specific terrain can further improve inchworm robot locomotion.

Acknowledgments

The authors express their gratitude to M. Škarytka and J. Bittner for their support during the testbed construction and to K. Kubíková for providing the real inchworm photography. The work has been supported by the Technology Agency of the Czech Republic under the project No. TN02000028 and by the European Union under the project ROBOPROX - Robotics and advanced industrial production (reg. no. CZ.02.01.01/00/22_008/0004590). The support under grant No. SGS23/184/OHK3/3T/13 to the second author is also gratefully acknowledged.

References

[1] D. Shen, Q. Zhang, C. Wang, X. Wang, and M. Tian, “Design and analysis of a snake-inspired crawling robot driven by alterable angle scales,” *IEEE Robotics and Automation Letters*, vol. 6, no. 2, pp. 3744–3751, 2021.

[2] *Scalybot: A Snake-Inspired Robot With Active Control of Friction*, ser. Dynamic Systems and Control Conference, vol. ASME 2011 Dynamic Systems and Control Conference and Bath/ASME Symposium on Fluid Power and Motion Control, Volume 2, 10 2011.

[3] A. Rafsanjani, Y. Zhang, B. Liu, S. M. Rubinstein, and K. Bertoldi, “Kirigami skins make a simple soft actuator crawl,” *Science Robotics*, vol. 3, no. 15, p. eaar7555, 2018.

[4] T. D. Ta, T. Umedachi, and Y. Kawahara, “Design of frictional 2d-anisotropy surface for wriggle locomotion of printable soft-bodied robots,” in *IEEE International Conference on Robotics and Automation (ICRA)*, 2018, pp. 6779–6785.

[5] F. Lamping, S. N. Gorb, and K. M. de Payrebrune, “Frictional properties of a novel artificial snakeskin for soft robotics,” *Biotribology*, vol. 30, p. 100210, 2022.

[6] M. M. Serrano, A. H. Chang, G. Zhang, and P. A. Vela, “Incorporating frictional anisotropy in the design of a robotic snake through the exploitation of scales,” in *IEEE International Conference on Robotics and Automation (ICRA)*, 2015, pp. 3729–3734.

[7] M. G. Selvamuthu, R. Tadakuma, N. Fujiwara, K. Yoshida, M. Takagi, H. Hoshino, Y. Suzuri, and H. Furukawa, “Development of soft inchworm robot with friction control of feet using double-network gel,” *Advanced Robotics*, vol. 37, no. 6, pp. 407–422, 2023.

[8] C. Tiner, S. Bapat, S. D. Nath, S. V. Atre, and A. Malshe, “Exploring convergence of snake-skin-inspired texture designs and additive manufacturing for mechanical traction,” *Procedia Manufacturing*, vol. 34, pp. 640–646, 2019.